



ELSEVIER

Available online at www.sciencedirect.com

SCIENCE @ DIRECT®

Journal of Magnetism and Magnetic Materials 293 (2005) 532–539

Journal of
magnetism
and
magnetic
materials

www.elsevier.com/locate/jmmm

Superparamagnetic colloid suspensions: Water magnetic relaxation and clustering

Alain Roch^a, Yves Gossuin^b, Robert N. Muller^a, Pierre Gillis^{b,*}

^aDepartment of Organic Chemistry and NMR Laboratory, University of Mons-Hainaut, B 7000 Mons, Belgium

^bBiological Physics Department, Université de Mons-Hainaut, Place du Parc, 20–B, 7000 Mons, Belgium

Available online 3 March 2005

Abstract

Ferrite superparamagnetic (SPM) nanoparticles in aqueous suspensions shorten the nuclear magnetic relaxation of water protons. For transverse relaxation, that effect is enhanced when agglomeration of elementary SPM cores occurs, because of an increase of the secular part of the transverse relaxivity. On the contrary, clustering weakens the T1-shortening, in agreement with the prediction of a new model for diffusion.

© 2005 Elsevier B.V. All rights reserved.

Keywords: MRI contrast agents; Nuclear magnetic relaxation dispersion; Clustering; Aggregation; Diffusion; Nanoparticles; T1 shortening; Magnetite; SPIO; USPIO

1. Introduction

Superparamagnetic (SPM) colloids improve the contrast in Magnetic Resonance Imaging (MRI). The particles currently used for this purpose are composed of very small individual ferrite crystals about 10 nm in diameter, stabilized by a polysaccharide or polyelectrolyte coating [1,2]. These particles are mainly used to shorten the transverse relaxation time. Their performances as contrast agent depend on parameters like size, clustering, magnetisation, and concentration.

SPM contrast agents are classified following their size: particles containing only one ferrite crystal are called ultra-small particles of iron oxide (USPIO), while relatively larger particles containing several magnetic crystals within the same flake of permeable coating are called small particles of iron oxide (SPIO) [3].

For USPIO, a theoretical approach assuming a uniform distribution of the magnetic crystals within the solvent is rather realistic and allows the calculation of the nuclear magnetic relaxation rate [4–6]. This assumption is no longer valid for SPIO, which contain several ferrite crystals per particle. The present work (experimental and theoretical) is aimed at accounting for the

*Corresponding author. Tel./fax: +32 65 37 35 37.

E-mail address: Pierre.gillis@umh.ac.be (P. Gillis).

agglomerated structure of SPIO, starting from the theory valid for USPIO.

Effects arising from the aggregation of magnetic grains are two-fold: on the one hand, those related to the global structure of the cluster and to the magnetic field distribution around it, and on the other hand, those limited to the inner part of the aggregate. While the former ones essentially affect T_2 and T_2^* [5,7], the latter ones govern T_1 .

We first remind the theoretical background allowing the interpretation of transverse relaxation induced by strongly magnetized inclusions [8], indicating a strong dependence of the relaxation rate with the particle radius. The transverse relaxivity, defined as the relaxation rate enhancement per millimole of iron, is studied through its dispersion with B_0 , the static field, and during a chemically induced agglomeration, the particle size being simultaneously measured by Photon Correlation Spectroscopy (PCS). Those measurements confirm the theoretical predictions.

Longitudinal relaxation is modeled by analyzing diffusion through the permeable coating of the agglomerate as a virtual exchange between normal decaying modes and bulk water. This model is in very good agreement with the flattening of the Nuclear Magnetic Relaxation Dispersion profiles during a chemically induced agglomeration of ferrite particles.

2. Theory

The cluster itself may be considered a large magnetized sphere whose total magnetic moment increases according to Langevin's law. The global magnetization of the agglomerate is always aligned on the external field. Its effect on relaxation is characterized by a long correlation time, because of its large size, so that its contribution mainly affects the secular term of the relaxation rate. This contribution is given by the outer sphere diffusion theory, provided the motional averaging condition is fulfilled: $\Delta\omega\tau_D < 1$, where $\Delta\omega$ is the difference in angular frequency between the local field experienced by a proton at the equatorial line of the cluster surface and in the bulk ($\Delta\omega = \mu_0 M\gamma/3$, where μ_0 is the vacuum magnetic permeability, M the particle magnetization, and γ the proton

gyromagnetic ratio); τ_D is the translational diffusion time around the cluster ($\tau_D = R_a^2/D$, R_a being the cluster radius and D the water diffusion coefficient) [8,9]:

$$1/T_2 = 16f_a \Delta\omega\tau_D/45 \quad (1)$$

with f_a the volume fraction occupied by the clusters. This secular contribution explains the increase of $1/T_2$ at high field [5,7]. Eq. (1) can be rewritten in order to make the cluster magnetic moment appear as

$$1/T_2 = (64\pi/135)[\mu_0\gamma\mu_{sp}N_gL(x)/(4\pi)]^2 \times N_A C_a/(R_a D), \quad (2)$$

where μ_{sp} is the magnetic moment of an elementary crystal, N_g is the number of crystals in an agglomerated particle, N_A is Avogadro's number, C_a is the agglomerate concentration in mmol/l, and $x = \mu_{sp}N_gB_0/(kT)$, B_0 being the static field, k the Boltzmann constant and T the temperature. The Langevin function $L(x)$ is defined as follows:

$$L(x) = \coth(x) - 1/x. \quad (3)$$

For aggregates with not too large sizes, usual echo times ($\tau_{CP} = TE/2$) are too long to be efficient, and there is no difference between T_2 and T_2^* .

When the motional averaging condition breaks down, T_2^* was shown to be given by the Static Dephasing Regime, which refers to the dephasing of motionless magnetic moments in a non-uniform field created by randomly distributed dipoles [10,11]:

$$1/T_2^* = 2\pi\sqrt{3}f_a\Delta\omega/9. \quad (4)$$

It applies to spheres with a radius large enough that $\tau_D > \tau_{SDR}$ [8], with

$$\tau_{SDR} = \pi\sqrt{3}/(2\Delta\omega). \quad (5)$$

T_2 remains equal to T_2^* as long as the refocusing pulses are not efficient. This only occurs for larger spheres, for diffusion times larger than τ_L , with

$$\tau_L = (1.49/\Delta\omega)x^{1/3}(1.52 + f_a x)^{5/3}, \quad (6)$$

where $x = \Delta\omega\tau_{CP}$.

For $\tau_D > \tau_L$, the relaxation rate decreases with the radius [8]:

$$1/T_2 = 1.8f_a x^{1/3}(1.52 + f_a x)^{5/3}/\tau_D \quad (7)$$

while T_2^* remains, given by Eq. (4).

The longitudinal relaxation rate does not contain any secular term, so that it goes to zero for frequencies larger than $1/\tau_c$, where τ_c is the correlation time of the fluctuation responsible for relaxation. Diffusion around the agglomerated particle is characterized by a correlation time too long to contribute significantly to the longitudinal magnetization recovery at usual imaging fields. Furthermore, at low field, i.e. for frequencies smaller than $1/\tau_c$, the global magnetic moment of the agglomerate is too weak to allow for a significant contribution to the longitudinal relaxation rate. For small agglomerates satisfying the motional averaging condition (for magnetite, the diameter must be smaller than 200 nm), the longitudinal relaxation rates arising from diffusion around the agglomerate are thus approximated by $1/T_{1a} \sim 0$. (8)

For SPIO, the assumption of a uniform distribution of the crystals within the whole suspension is obviously abandoned, and is replaced by the assumption of a uniform distribution of the elementary crystals within a permeable coating flake, which is the agglomerated particle.

We will rest on a formal analogy between our diffusion problem and a chemical exchange situation. In a system where there is fast exchange of water between a bulk fraction, containing the majority of the solvent molecules, and an ensemble of bound fractions, each characterized by a chemical shift and a fast intrinsic relaxation, the probability that a molecule attached to one of the binding sites at $t = 0$, will still be attached to the same site at time t , decays exponentially with t . The longitudinal relaxation rate calculated in such a situation is [12]

$$1/T_1 = 1/T_1^b + \sum_n \frac{f_n}{\tau_n + T_1^n}, \quad (9)$$

where T_1^b is the relaxation time in the bulk fraction, f_n is the water fraction occupying site n ($f_n \ll 1$), τ_n is the residence time on site n , and T_1^n is the relaxation time on site n .

If $W(\vec{r}, t)$ is the density of probability for a water proton to be at point \vec{r} at time t , the evolution of this probability is governed by

the diffusion equation

$$\partial W(\vec{r}, t)/\partial t = D\Delta W(\vec{r}, t). \quad (10)$$

$\vec{r} = 0$ corresponds to the center of the spherical agglomerate. At $t = 0$, the water molecule is supposed to be somewhere within the agglomerate with a radius R_a , so that

$$W(\vec{r}, 0) = 0 \quad \text{if } |\vec{r}| > R_a,$$

$$W(\vec{r}, 0) = 3/(4\pi R_a^3) \quad \text{if } |\vec{r}| \leq R_a. \quad (11)$$

The space where the molecules are allowed to diffuse is much larger than the agglomerate itself. If we consider this space as a larger sphere of radius R_e , in order to avoid breaking the spherical symmetry of the problem (R_e is then half the mean distance between two agglomerates, $R_e/R_a = (\pi/6f_a)^{1/3}$), the solution of Eq. (10), starting from the initial conditions given in Eq. (11), may be written as:

$$W(r, t) = \frac{3}{2\pi R_a R_e r} \sum_{n=1}^{\infty} B_n \sin(n\pi r/R_e) e^{-n^2\pi^2 D t/R_e^2}, \quad (12)$$

where $B_n = [\sin \alpha_n/\alpha_n - \cos \alpha_n]/\alpha_n$, with $\alpha_n = n\pi R_a/R_e$. Using the definition $\tau_n = R_e^2/(n^2\pi^2 D) = \tau_D/\alpha_n^2$, Eq. (12) may be read as if at time $t = 0$, each decaying mode appearing in the solution of the diffusion equation, with a decay time τ_n , would be a virtual water fraction with a relative population (excluding the water outside the agglomerate) given by

$$p_n = \frac{6R_a}{R_e} B_n^2, \quad (13)$$

leaving site n at a rate equal to $1/\tau_n$. The factor p_n in Eq. (13) was obtained by integrating $W(r, 0)$ over a sphere of radius R_a ; it has a maximum for $\alpha_n = 2.082$, which corresponds to a decay time $\tau_n = 0.23\tau_D$ (see Fig. 1). The most populated mode is thus characterized by a decay time close to the exchange time that has to be used if the transverse relaxation time due to diffusion is described with a chemical exchange model ($\tau_{ex} = 0.26\tau_D$) [13].

In order to transfer these results into Eq. (9), we need noting that f_n , the relative amount of each “fraction”, is equal to $f_a p_n$. The intrinsic relaxation time in any fraction n , called T_1^n , is obtained from

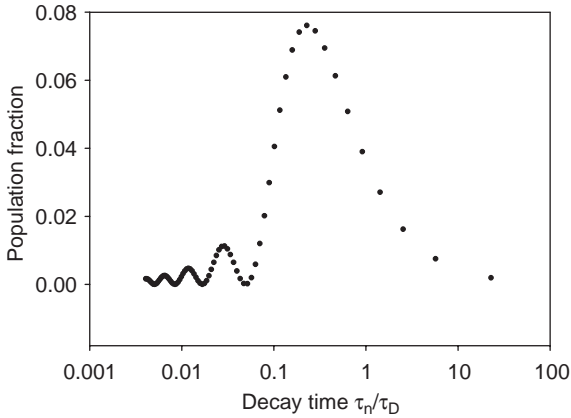


Fig. 1. Display of the relative fractions associated to the diffusion modes (Eq. (13)), expressed as a function of the ratio of the decay time over the diffusion time (τ_n/τ_D) for $R_c/R_a = 15$.

the theory valid for USPIO [5], and is expressed assuming a relaxivity r_1^g ($1/T_1^g = C_g r_1^g$, where C_g is the iron molar concentration within the aggregate). Given that C , the total iron concentration, is equal to $f_a C_g$, we finally get

$$1/T_1 = 1/T_1^b + C \sum_{n=1}^{\infty} \frac{P_n}{1/r_1^g + C_g \tau_n}. \quad (14)$$

Fig. 2 is the theoretical prediction from Eq. (14). The USPIO relaxivity r_1^g depends on several parameters characterizing the elementary grains embedded in the coating, namely their radius, their saturation magnetization (M_S), and the Néel relaxation time, typical of superparamagnetism (τ_N). These parameters were adjusted in order to fit the experimental curve corresponding to an agglomerate of 50 nm in radius shown in Fig. 5. The best values were 8.2 nm for the grain radius, $\tau_N = 1.8$ ns, $M_S = 49$ uem/(g Fe), and a volume fraction occupied by the ferrite crystals inside the agglomerate of 0.02.

3. Material and methods

Transverse relaxation rates were measured on suspensions of dextran coated magnetite particles called AMI25, delivered by Advanced Magnetics (Cambridge, MA, USA).

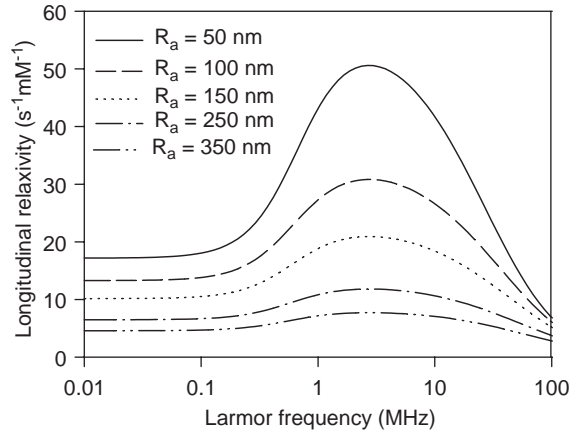


Fig. 2. Theoretical longitudinal NMRD profiles from Eq. (14). The parameters characterizing the elementary grains are given in the text.

The field dispersion of the transverse relaxivity was measured by means of three low field spectrometers working, respectively, at Larmor proton frequencies of 10, 20 and 40 MHz (Minispec Bruker PC110, PC120 and PC140), with CPMG sequences.

Agglomeration was caused by submitting the particles to an acid environment, destroying the dextran coating progressively. The particles were put in a phosphate buffer (NaH_2PO_4 1 M, pH = 4). Measurements of the cluster size were performed by PCS (Brookhaven Instrument Corporation BI-160, Holtsville, New York, USA), and during the same process, transverse relaxivity was recorded on a Minispec Bruker PC120 ($B_0 = 0.47$ T) with an echo time 0.7 ms ($\tau_{CP} = 0.35$ ms). Measurements were made at $T = 37^\circ\text{C}$.

The effect of agglomeration on longitudinal relaxation times was studied on suspensions of manganese zinc ferrites coated with anionic polyacrylate, synthesized by Dr K. Korman, BASF. A controlled flocculation of these coated manganese zinc ferrites was induced by adding Ca^{++} counterions to the suspension. The agglomeration kinetics was also followed by measurement of the size by PCS. Water proton longitudinal relaxation rates were measured at different stages of agglomeration using an IBM research field cycling relaxometer

(IBM Research, Yorktown Heights, New York, USA). This relaxometer is designed to provide NMRD profiles, i.e. measurements of the solvent proton longitudinal relaxation rate as a function of the static magnetic field.

4. Results and discussion

Transverse relaxation: Fig. 3 clearly shows that the measured relaxivity is much larger than expected from the sole contribution arising from the inner part of the aggregate (dotted line). Adding a contribution due to diffusion around the whole aggregate allows reproducing the steep increase of relaxivity at high field, although the saturation of this increase predicted by the theory is not confirmed by the experimental measurements. This saturation could be masked by a possible surface contribution, with a paramagnetic behavior. The volume ratio of ferrite in the agglomerate was adjusted to fit the experimental results.

Fig. 4 shows that the relaxivity first decreases under the dextran chemical destruction, probably

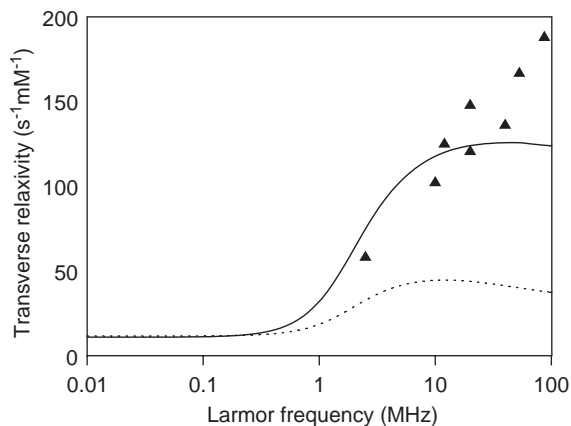


Fig. 3. Transverse relaxivity of AMI25 samples. The triangles are experimental data. The dotted line is the prediction from USPIO theory (without accounting for agglomeration), with the grain parameters obtained from the fitting to Eq. (14) of the longitudinal relaxivity for $R_a = 120$ nm (from PCS measurements) in Fig. 5 (grain radius: 6.4 nm, specific magnetization: 41 emu/(g Fe) and Néel relaxation time: 1.8 ns). The solid line is obtained by adding the contribution given in Eq. (2), with a volume ratio of ferrite in the agglomerate of 0.032.

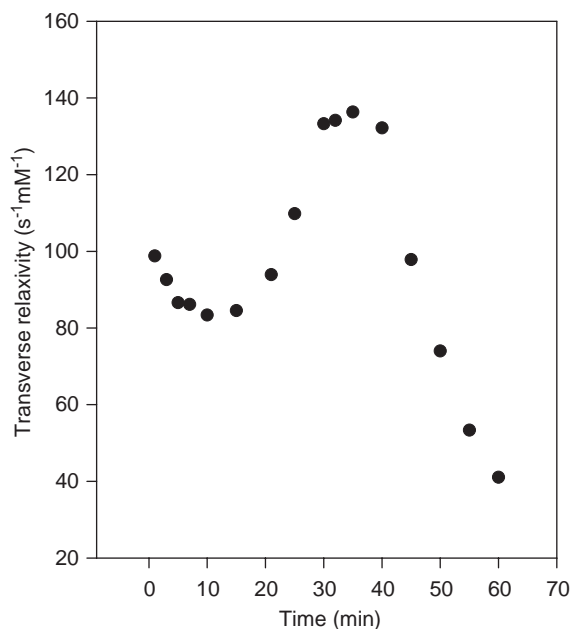


Fig. 4. Evolution of the transverse relaxivity of an AMI 25 sample, during the clustering process induced by a phosphate buffer (pH = 4), at a proton Larmor frequency of 20 MHz, $TE = 0.7$ ms, $T = 37$ °C.

because of an initial breaking of the already partially agglomerated particles, in a situation where coating remains sufficient to prevent further agglomeration. The following increase of the relaxivity is assigned to clustering, leading to a plateau. Theory also predicts the existence of a plateau, for τ_D ranging from τ_{SDR} (Eq. (5)) to τ_L (Eq. (6)) [8]; the experiment presented here is the first experimental confirmation of the theory, as far as the existence of a size domain where T_2 is not different from the SDR T_2^* is concerned. The Static Dephasing Regime (Eq. (4)) previously provided the basis for a method aimed at determining iron-oxide concentration *in vivo*, using $R_2 = R_2^* - R_2$ measurements [14].

The relaxivity at the plateau is $134 \text{ s}^{-1}(\text{mM Fe})^{-1}$, which can be used to deduce the value of $\Delta\omega$, from Eq. (4); given the magnetite volumic mass (5100 kg/m^3) and its chemical composition (Fe_3O_4), we have $f_a = 1.52 \times 10^{-5} [\text{Fe}]$, where $[\text{Fe}]$ is the iron concentration given in millimol per liter. The relaxivity is defined as the relaxation rate for $[\text{Fe}] = 1 \text{ mmol Fe/l}$. We thus deduce $\Delta\omega = 7 \cdot 29 \times$

10^6 rad/s, which corresponds to a magnetization 6.5×10^4 A/m. This result is 14% of the magnetite bulk magnetization (4.8×10^5 A/m). Introduced into Eq. (5), we get $\tau_{SDR} = 3.73 \times 10^{-7}$ s, and finally, if $D = 3 \times 10^{-9}$ m²/s, $R_a = 33$ nm at the left edge of the plateau.

The relaxivity plateau's right edge is theoretically given by Eq. (6), with $x = 2550$: $\tau_L = 5.85 \times 10^{-6}$ s, and thus $R_a = 132.5$ nm. Comparing those results with the PCS measurements is rather satisfying: the relaxivity plateau is reached for times between 30 and 40 min, the corresponding radii (half the measured size) ranging during the same time interval from 100 to 125 nm (see Fig. 5). The agreement between the sizes measured by PCS and the theoretical estimations is reasonable, especially if considering the weak precision of the PCS measurements during the initial stage of the agglomeration process.

Longitudinal relaxation: Because of the polyacrylate coating, the particles are negatively charged, which prevents them to approach one another. The Ca^{++} divalent cations neutralize the carboxyl anions, and the negative electric charge on the coating decreases down to the vanishing of the repulsive forces responsible for the stability of the solution. Fig. 6 shows the agglomeration

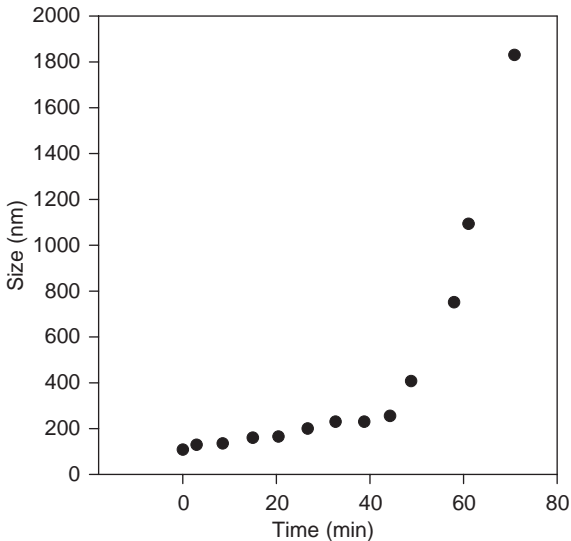


Fig. 5. Evolution of the hydrodynamic size of the same sample as in Fig. 4.

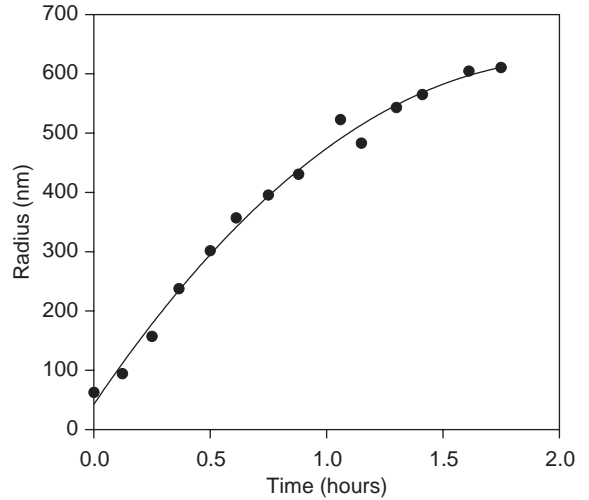


Fig. 6. Evolution of the hydrodynamic size, as measured by PCS, during the Ca^{2+} induced agglomeration.

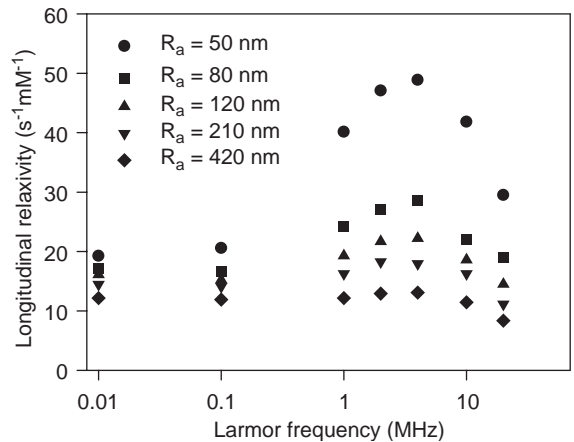


Fig. 7. Evolution of the experimental NMRD profiles during agglomeration ($T = 37^\circ C$). The sizes indicated on the figure are determined according to the mean measurement time, using the data of Fig. 4.

kinetics of the zinc ferrite coated with polyacrylate induced by addition of Ca^{++} counter-ions to the suspension.

NMRD profiles also evolve with clustering (see Fig. 7): the profiles become flatter on increasing agglomeration. Comparison of the clustering-dependent experimental curves with the theoretical ones (Fig. 2) shows the adequacy of our modeling

with the physical and morphological properties of clustered SPM colloids. However, one can remark that the flattening of the longitudinal relaxivity profile is more pronounced than predicted: for instance, going from $R_a = 50$ to 100 nm reduces the amplitude of the relaxivity peak by a factor of 2 on Fig. 7 (experimental results), but only by a factor of 1.6 on Fig. 2 (theoretical predictions from Eq. (14)). This discrepancy is likely to be due to a questionable implicit theoretical assumption— C_g , the concentration of the crystals within the agglomerates, was supposed to be invariant during the agglomeration process, and the same value was used to draw all the curves presented in Fig. 2. However, the effect of the Ca^{++} ions, i.e. decreasing the repulsive forces between the crystals, not only increases the size of the agglomerates, but also allows the crystals to get closer to each other, which in turn increases the concentration in the agglomerate. Now, Eq. (14) clearly shows that increasing C_g , with all other variables being unchanged, will decrease the relaxation rate.

The success of our modeling is somehow surprising because the assumption of a uniform distribution of ferrite crystals is far from realistic: the structures known to minimize the magnetic energy of associated ferrite crystals are shaped as rings or open loops [15]. The good agreement between the predictions of our simple model and the experimental results is therefore an indication that the distribution of the elementary grains within the aggregates does not play a critical role regarding relaxation.

5. Conclusion

This work unambiguously demonstrates that accounting for agglomeration is mandatory for explaining the relaxation properties of SPM colloids. Published theoretical models [4–6] do not incorporate such a feature: they only apply to non-agglomerated suspensions, the so-called US-PIO, where each flake does not generally contain more than one ferrite crystal. Agglomeration modifies longitudinal as well as transverse relaxation, but in very different ways. Considering the entire agglomerate as a single magnetized entity

accounts for the observed increase of the transverse relaxation rate at high field. However, the classical outer-sphere theory only provides a very crude and semi-quantitative approximation of its value. A more accurate calculation of this contribution probably requires further recourse to numerical methods described elsewhere [7,16]. Furthermore, the three regimes theoretically predicted (outer sphere, with a relaxation rate increasing with τ_D ; static dephasing, characterized by a plateau as a function of τ_D ; echo limited, with a relaxation rate inversely proportional to τ_D) were successively met during a chemically induced clustering process.

Longitudinal relaxation undergoes quite different modifications under agglomeration: NMRD profiles become flatter, because of an important decrease of the relaxation rates. This effect is interpreted as the result of a virtual exchange between the water inside the agglomerates, rapidly relaxed, and the waters within the bulk, relaxing much slower. The time spent by the water molecules within the agglomerate is not simply given by the usual diffusion time $\tau_D = R_a^2/D$, it is instead deduced from the exact solution of the diffusion equation in a finite spherical space, producing an ensemble of decaying modes each characterized by its own decay time. These modes play the same role as binding sites with a short relaxation time, and with a residence time corresponding to the decay time of the diffusion modes (Fig. 7).

This model is shown to reproduce the decrease of the longitudinal relaxivity observed during a chemically induced agglomeration process. For small-size aggregates ($R_a < 50$ nm) in pure water, this phenomenon is often masked behind an underestimation of the saturation magnetization, fitted to a value lower than the magnetometric direct measurement.

References

- [1] R.L. Magin, G. Bacic, M.R. Niesman, et al., *Magn. Reson. Med.* 20 (1991) 1.
- [2] G. Mair, W. Steck, US Patent Application No. 4,810 (1989) 401.

- [3] R.N. Muller, A. Roch, J.M. Colet, et al., Particulate magnetic contrast agents, in: A.E. Merbach, E. Toth (Eds.), *The Chemistry of Contrast Agents in Medical Magnetic Resonance Imaging*, Wiley, Chichester, 2001.
- [4] A. Roch, R.N. Muller, *Proceedings of the 11th Annual Meeting of the Society of Magnetic Resonance in Medicine, Works in Progress*, 1992, p.1447.
- [5] A. Roch, R.N. Muller, P. Gillis, *J. Chem. Phys.* 110 (1999) 5403.
- [6] A. Roch, R.N. Muller, P. Gillis, *J. Magn. Reson. Imag.* 14 (2001) 94.
- [7] F. Moiny, P. Gillis, A. Roch et al., *Proceedings of the 11th Annual Meeting of the Society of Magnetic Resonance in Medicine, Works in Progress*, 1992, p.1431.
- [8] P. Gillis, F. Moiny, R.A. Brooks, *Magn. Reson. Med.* 47 (2002) 257.
- [9] Y. Ayant, E. Belorizky, J. Alizon, J. Gallice, *J. Phys.* 36 (1975) 991.
- [10] R.J.S. Brown, *Phys. Rev.* 121 (1961) 1379.
- [11] D.A. Yablonskiy, E.M. Haacke, *Magn. Reson. Med.* 32 (1994) 749.
- [12] J.R. Zimmerman, W.E. Brittin, *J. Chem. Phys.* 61 (1957) 1328.
- [13] R.A. Brooks, F. Moiny, P. Gillis, *Magn. Reson. Med.* 45 (2001) 1014.
- [14] C.V. Bowen, X. Zhang, G. Saab, et al., *Magn. Reson. Med.* 48 (2002) 52.
- [15] R.W. Chantrell, A. Bradbury, et al., *J. Appl. Phys.* 53 (1982) 2742.
- [16] R.M. Weisskoff, C.S. Zuo, et al., *Magn. Reson. Med.* 31 (1994) 601.